

A templated synthesis of tetranuclear polyoxoalkoxymolybdates(v). Bromo coordinated oxomolybdenum(v) clusters: known core structure with new ligands. Oxidation to the Lindquist anion

Barbara Modec,^{*a} Jurij V. Brenčič^a and Jon Zubieta^b

^a Faculty of Chemistry and Chemical Technology, University of Ljubljana, Aškerčeva 5, 1000 Ljubljana, Slovenia. E-mail: barbara.modec@uni-lj.si

^b Department of Chemistry, Syracuse University, New York 13244, USA. E-mail: jazubiet@mailbox.syr.edu

Received 6th November 2001, Accepted 25th January 2002

First published as an Advance Article on the web 11th March 2002

Reactions of (PyH)₂[MoOCl₅] and (PyH)[MoOBr₄] with alcohols in the presence of tetramethylpyrazine have inadvertently resulted in a series of tetranuclear polyoxoalkoxymolybdates(v) with the general formula (PyH)₂-[Mo₄O₈(OR)₂(HOR)₂X₄] (**1a**: R = Me, X = Cl; **1b**: R = Et, X = Cl; **1c**: R = Et, X = Br). Reaction with the nitrogen donor ligand pyridine (Py = C₅H₅N), run under similar conditions, afforded neutral cluster [Mo₄O₈(OEt)₂Br₂Py₄] **2a**, which also crystallizes as an acetonitrile solvate, [Mo₄O₈(OEt)₂Br₂Py₄]·2CH₃CN **2b**. The compounds were characterized by single crystal X-ray diffraction studies. All five tetranuclear clusters contain as a common feature the {Mo₄O₄-(μ₃-O)₂(μ-O)₂(μ-OR)₂}²⁺ core onto whose periphery different terminal ligands are attached. The core structure may be viewed as the fusion of two well-defined {Mo₂O₄}²⁺ building blocks bridged through oxo groups. The {Mo₂O₄}²⁺ clusters with coordinated bromo ligands are the first of this type to be structurally characterized. Introduction of water resulted in a fully oxidized [LH₂][Mo₆O₁₉]·L·2EtOH **3** (L = tetramethylpyrazine) whose structure consists of Lindquist anions trapped in the vacancies between the intertwined organic chains with the LH₂²⁺ ··· ethanol ··· L repeating unit.

Introduction

The coordination chemistry of polyoxometalates is an area of increasing interest owing to the structural analogy of these species to the parent metal oxides. The interest derives from the expectation that their chemistry will provide some insight into the mechanisms of the catalytic processes taking place on the surface of the solid metal oxide.¹

The {Mo₂O₄}²⁺ fragment (Fig. 1) with d-electrons localized in

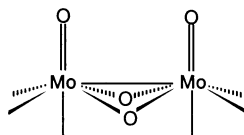


Fig. 1 {Mo₂O₄}²⁺: A basic building unit of oxomolybdenum(v) clusters.

a Mo(v)–Mo(v) single bond appears as a recurrent structural motif in a number of molecular systems.² Examples of some structurally characterized compounds include: an organometallic complex [(C₅Me₅Rh)₈(Mo^{VI}O₄)(Mo₁₂O₃₆)]²⁺,³ and coordination compounds employing a large variety of ligands *i.e.* [4-MeC₅H₄NMe₂]₂[Mo₂O₄(cbdt)₂] (cbdt = 1,2-dicarba-*closo*-dodecaborane-1,2-dithiolate),⁴ [Mo₄O₆(OEt)₄Cl₄(PMe₃)₂],⁵ [Mo₄O₈(OMe)₂Cl₂Py₄], [Mo₆O₁₂(OMe)₆Py₄],⁶ [Mo₈O₁₆(OMe)₈(PMe₃)₄]⁷ and [(Mo^{VI}O₃)₄Mo₁₂O₂₈(OH)₁₂]^{8–8}. The complexity of their stoichiometries blurs their structural interrelationships, yet upon careful inspection essentially isostructural single {Mo₂O₄}²⁺ units or the aggregates of two, three, four or more dimers can be recognized in all. The geometry of the {Mo₂O₄}²⁺ unit is seen to remain unaffected by the nature of other ligands which complete the metal's coordination sphere.

When compared to the oxomolybdate(vi) chemistry, where the infinite chain, sheet or lattice framework structures find

frequent occurrence,^{2a} the structural chemistry of oxomolybdenum(v) compounds is limited, with the exception of two examples, to the finite oxomolybdenum(v) core structures. With the recently prepared polymeric [Mo₂O₂As₂S₇]²⁻ and [Mo₂O₂As₂Se₇]²⁻ where {Mo₂O₂(μ-S)₂}²⁺ or {Mo₂O₂(μ-Se)₂}²⁺ dimers, thio or seleno derivatives of {Mo₂O₄}²⁺, are connected with [As₂Q₅]⁴⁻ (Q = S, Se) ligands, the idea of extended oxomolybdenum(v) structures based on the {Mo₂O₂(μ-E)₂}²⁺ (E = O, S, Se) building blocks linked with suitable bridging ligands has been realized for the first time.⁹ Our interest has recently focused on pyrazine and its alkyl substituted derivatives for several reasons. Pyrazine is well-known to act as a linking ligand.¹⁰ Not surprisingly, the only two structurally characterized oxomolybdenum compounds with pyrazine, both with the [MoO₃(Pyz)_{1/2}] composition, turn out to be polymeric oxomolybdenum(vi) compounds.¹¹ Using the alcoholic solution of tetramethylpyrazine and mononuclear oxohalomolybdates(v) as starting materials has resulted in a series of tetranuclear polyoxoalkoxymolybdates(v) with the (PyH)₂[Mo₄O₈(OR)₂-(HOR)₂X₄] composition. The role of the N,N-bidentate ligand evolved to that of a structure directing agent, instead the oxygen donor ligands, alcohol and the *in situ* produced alkoxide, were incorporated into the cluster. We also wish to report here the syntheses and the structures of another tetranuclear cluster, a neutral [Mo₄O₈(OEt)₂Br₂Py₄] with coordinated pyridine, and of the oxidized cluster, [LH₂][Mo₆O₁₉]·L·2EtOH (L = tetramethylpyrazine).

Experimental

General techniques

Acetonitrile, ethanol, methanol, pyridine and tetramethylpyrazine were purchased from Aldrich and used without further purification.

The starting oxohalomolybdates(v), $(\text{PyH})_2[\text{MoOCl}_5]$ and $(\text{PyH})[\text{MoOBr}_4]$, were prepared according to literature methods.¹²

The infrared spectra were measured on solid samples as Nujol or poly(chlorotrifluoroethylene) mulls using a Perkin-Elmer 2000 Fourier Transform infrared spectrometer. Elemental analyses were carried out by the Chemistry Department service at the University of Ljubljana. Molybdenum was determined as PbMoO_4 and halide by potentiometric titration with a 0.100 M solution of AgNO_3 .

Preparations

$(\text{PyH})_2[\text{Mo}_4\text{O}_8(\text{OMe})_2(\text{HOMe})_2\text{Cl}_4]$ 1a. Tetramethylpyrazine (140 mg, 1.028 mmol) was dissolved in methanol (5 cm^3), and $(\text{PyH})_2[\text{MoOCl}_5]$ (300 mg, 0.668 mmol) was added. The resulting solution, of deep orange colour, was allowed to stand at ambient conditions for three days. The orange crystalline product was collected and washed with hexanes. Yield 65 mg (41%). Calc. for $\text{C}_{14}\text{H}_{26}\text{Cl}_4\text{Mo}_4\text{N}_2\text{O}_{12}$: C, 17.89; H, 2.79; Cl, 15.09; Mo, 40.83; N, 2.98. Found: C, 17.79; H, 2.83; Cl, 14.90; Mo, 40.60; N, 2.85%. IR (cm^{-1}): 3223m, 3130w, 3088w, 3062w, 2950w, 2932w, 2831w, 1636s, 1611s, 1538s, 1252m, 1202s, 1164s, 1113m, 1033vvs, 1002vvs, 966vvs, 946vvs, 756vvs, 725vvs, 679vvs, 609s, 516vs, 492vvs, 390s, 348m, 318s, 301m, 283m, 236w and 209w.

$(\text{PyH})_2[\text{Mo}_4\text{O}_8(\text{OEt})_2(\text{HOEt})_2\text{Cl}_4]$ 1b. Tetramethylpyrazine (70 mg, 0.514 mmol) was dissolved in the mixture of ethanol (5 cm^3) and acetonitrile (2.5 cm^3). $(\text{PyH})_2[\text{MoOCl}_5]$ (60 mg, 0.134 mmol) was added, and the resulting solution was allowed to stand at ambient conditions. The orange crystalline product which formed within a short time was collected after one day and washed with hexanes. Yield 24 mg (72%). Calc. for $\text{C}_{18}\text{H}_{34}\text{Cl}_4\text{Mo}_4\text{N}_2\text{O}_{12}$: C, 21.71; H, 3.44; Cl, 14.24; Mo, 38.53; N, 2.81. Found: C, 21.44; H, 3.15; Cl, 14.00; Mo, 38.35; N, 2.74%. IR (cm^{-1}): 3217m, 3132w, 3080w, 3059w, 2980m, 2930w, 2888w, 1636m, 1614m, 1543m, 1254m, 1203m, 1166w, 1157w, 1087s, 1033vs, 969vvs, 946vs, 885s, 761s, 727vvs, 681vvs, 610m, 522m, 497s, 471m, 394w, 325s, 276m, 235m and 206m.

$(\text{PyH})_2[\text{Mo}_4\text{O}_8(\text{OEt})_2(\text{HOEt})_2\text{Br}_4]$ 1c. *Procedure a.* Tetramethylpyrazine (22.5 mg, 0.165 mmol) was dissolved in ethanol (5 cm^3). $(\text{PyH})[\text{MoOBr}_4]$ (75 mg, 0.147 mmol) was added, and the resulting solution was allowed to stand at ambient conditions overnight. The orange crystalline product was collected and washed with hexanes. Yield 23 mg (53%).

Procedure b. $(\text{PyH})[\text{MoOBr}_4]$ (500 mg, 0.977 mmol) was dissolved in acetonitrile (20 cm^3). After the transfer of the orange solution into an Erlenmeyer flask, a small container filled with the mixture of ethanol (9.5 cm^3) and pyridine (0.5 cm^3) was carefully inserted into the flask. The flask was stoppered and the solvents were allowed to mix by vapour diffusion. Yellow crystalline product, obtained after four days, was collected and washed with hexanes. Yield 45 mg (16%). Calc. for $\text{C}_{18}\text{H}_{34}\text{Br}_4\text{Mo}_4\text{N}_2\text{O}_{12}$: C, 18.42; H, 2.92; Br, 27.23; Mo, 32.69; N, 2.39. Found: C, 18.60; H, 2.70; Br, 27.00; Mo, 32.45; N, 2.16%. IR (cm^{-1}): 3218s, 3132w, 3079m, 3057m, 2980m, 2928w, 2887w, 1636m, 1616m, 1546m, 1253w, 1203w, 1164w, 1156w, 1085s, 1030vs, 968vvs, 946vs, 881s, 759m, 725vvs, 682vs, 669vs, 610m, 521m, 493s, 467m, 388w, 359sh, 310s, 285sh, 241m and 204m.

Note. The compounds **1a**, **1b** and **1c** were found to decompose on prolonged exposure to the air.

$[\text{Mo}_4\text{O}_8(\text{OEt})_2\text{Br}_2\text{Py}_4]$ and $[\text{Mo}_4\text{O}_8(\text{OEt})_2\text{Br}_2\text{Py}_4]\cdot 2\text{CH}_3\text{CN}$, **2a and **2b.** $(\text{PyH})[\text{MoOBr}_4]$ (500 mg, 0.977 mmol) was dissolved in acetonitrile (20 cm^3). After the transfer of the orange solution into an Erlenmeyer flask, a small container filled with a mixture of ethanol (5 cm^3) and pyridine (5 cm^3) was carefully inserted into the flask. The flask was stoppered and the solvents were allowed to mix by vapour diffusion. Red crystalline**

product, obtained after five days, was collected. It contained three phases: dark red, block-shaped crystals of **2a**, orange plate-like crystals of **2b** and red, hexagon-shaped crystals which turned opaque almost immediately when removed from the mother liquor. The IR spectrum of the dried sample of the latter was shown to be identical with the IR spectrum of the stable $[\text{Mo}_4\text{O}_8(\text{OEt})_2\text{Br}_2\text{Py}_4]$ **2a**. Yield 160 mg (61%). Calc. for $\text{C}_{24}\text{H}_{30}\text{Br}_2\text{Mo}_4\text{N}_4\text{O}_{10}$: C, 26.74; H, 2.80; N, 5.20. Found: C, 26.96; H, 3.05; N, 5.31%. IR (cm^{-1}): 2960w, 2924m, 2850w, 1608s, 1220s, 1158m, 1092w, 1072s, 1048s, 1033s, 1017s, 963vs, 942s, 884m, 757m, 737s, 691s, 667vs, 496s, 316m and 253w.

$[\text{LH}_2][\text{Mo}_6\text{O}_{19}]\cdot \text{L}\cdot 2\text{EtOH}$ 3. The same procedure was used as for the synthesis of **1b**. No $(\text{PyH})_2[\text{Mo}_4\text{O}_8(\text{OEt})_2(\text{HOEt})_2\text{Cl}_4]$ **1b** was obtained, instead the colour of the solution changed to blue green. The crystalline product, of a light yellow colour, was obtained after several days.

Note. To promote the oxidation to Mo(vi) a drop of water (*ca.* 0.05 cm^3) was added to the final reaction mixture. The originally orange solution changed colour to blue green within 3 to 7 days. The colour change was accompanied with precipitation of a yellow white crystalline product, **3**. Yield 4 mg (29%). This reaction was repeated several times and the yields were reproducible.

No elemental analysis was performed since the crystals quickly lost the ethanol solvent of crystallization when removed from the solution. IR (cm^{-1}): 3162w, 2923w, 1644m, 1218m, 1154w, 1096m, 1047m, 999s, 957vvs, 878w, 799vvs, 720vvs, 601m, 431m and 354m.

Crystallography

Data were collected on Bruker SMART CCD (compound **1a**), Enraf Nonius CAD-4 (compound **1b**) and Nonius Kappa CCD (compounds **1c**, **2a**, **2b** and **3**) diffractometers using monochromated Mo-K α radiation [$\lambda = 0.71073 \text{ \AA}$]. Crystals were either sealed in a Lindemann capillary (**1b**) or else directly mounted on the diffractometer under a stream of cold nitrogen gas. The absorption corrections were applied only for **1a** and **1b**: an empirical absorption correction (SADABS)¹³ for **1a** and the ψ -scan method for **1b**.¹⁴ The structures were solved¹⁵ by direct methods and refined¹⁵ on F^2 by full-matrix least squares with anisotropic displacement parameters for the non-hydrogen atoms. Figures depicting the structures were prepared using SHELXTL¹⁶ and PLATON.¹⁷ Crystal and data collection parameters are given in Tables 1 and 2.

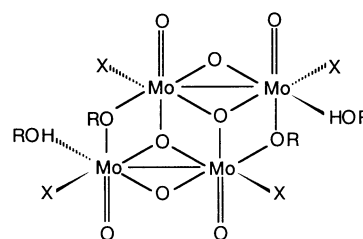
CCDC reference numbers 173626–173631.

See <http://www.rsc.org/suppdata/dt/b1/b110062a/> for crystallographic data in CIF or other electronic format.

Results and discussion

Structural studies

The crystal structures of $(\text{PyH})_2[\text{Mo}_4\text{O}_8(\text{OR})_2(\text{HOR})_2\text{X}_4]$ **1a**, **1b** and **1c**. The structures of $(\text{PyH})_2[\text{Mo}_4\text{O}_8(\text{OR})_2(\text{HOR})_2\text{X}_4]$, **1a**, **1b** and **1c** are very similar (see Scheme 1). They consist of



- 1a** R = Me, X = Cl
1b R = Et, X = Cl
1c R = Et, X = Br

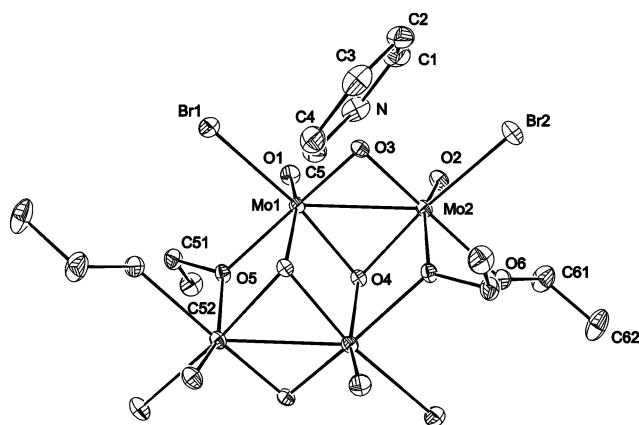
Scheme 1 Structures of **1a-c**.

Table 1 Crystallographic data for compounds **1a**, **1b** and **1c**

	1a	1b	1c
Empirical formula	C ₁₄ H ₂₆ Cl ₄ Mo ₄ N ₂ O ₁₂	C ₁₈ H ₃₄ Cl ₄ Mo ₄ N ₂ O ₁₂	C ₁₈ H ₃₄ Br ₄ Mo ₄ N ₂ O ₁₂
Formula weight	939.9	996.0	1173.9
Crystal system	Triclinic	Triclinic	Triclinic
Space group	<i>P</i> $\bar{1}$	<i>P</i> $\bar{1}$	<i>P</i> $\bar{1}$
<i>T</i> /K	150(2)	293(2)	200(2)
<i>a</i> /Å	9.0503(9)	9.1930(10)	9.21240(10)
<i>b</i> /Å	9.2675(9)	9.7236(9)	9.84160(10)
<i>c</i> /Å	9.7103(9)	10.441(2)	10.43200(10)
<i>a</i> °	109.404(2)	110.690(10)	110.8365(6)
<i>β</i> °	110.841(2)	104.24(2)	104.1747(6)
<i>γ</i> °	98.077(2)	100.200(10)	99.9521(6)
<i>V</i> /Å ³	686.30(11)	809.63(19)	821.026(15)
<i>Z</i>	1	1	1
<i>μ</i> /mm ⁻¹	2.232	1.898	6.414
Collected reflections	4663	5069	7160
Unique reflections, <i>R</i> _{int}	3166, 0.0181	3882, 0.0122	3742, 0.0206
Observed reflections	2711	3387	3237
<i>R</i> 1 [<i>I</i> > 2σ(<i>I</i>)]	0.0289	0.0237	0.0256
<i>wR</i> 2 (all data)	0.0778	0.0637	0.0576

Table 2 Crystallographic data for compounds **2a**, **2b** and **3**

	2a	2b	3
Empirical formula	C ₂₄ H ₃₀ Br ₂ Mo ₄ N ₄ O ₁₀	C ₂₈ H ₃₆ Br ₂ Mo ₄ N ₆ O ₁₀	C ₂₀ H ₃₈ Mo ₆ N ₄ O ₂₁
Formula weight	1078.1	1160.2	1246.2
Crystal system	Monoclinic	Triclinic	Triclinic
Space group	<i>P</i> ₂ / <i>c</i>	<i>P</i> $\bar{1}$	<i>P</i> $\bar{1}$
<i>T</i> /K	293(2)	150(2)	200(2)
<i>a</i> /Å	13.8953(3)	12.4794(2)	8.66390(10)
<i>b</i> /Å	16.9472(4)	12.7579(1)	10.8201(10)
<i>c</i> /Å	14.4907(3)	13.5427(2)	11.05740(10)
<i>a</i> °	90	67.5773(5)	77.6940(4)
<i>β</i> °	98.3770(10)	82.6479(5)	67.0360(4)
<i>γ</i> °	90	70.4822(5)	67.1440(4)
<i>V</i> /Å ³	3375.96(13)	1878.60(4)	877.163(15)
<i>Z</i>	4	2	1
<i>μ</i> /mm ⁻¹	3.874	3.491	2.168
Collected reflections	13525	14962	7765
Unique reflections, <i>R</i> _{int}	7607, 0.0250	8344, 0.0236	4020, 0.0134
Observed reflections	5919	7487	3608
<i>R</i> 1 [<i>I</i> > 2σ(<i>I</i>)]	0.0480	0.0402	0.0218
<i>wR</i> 2 (all data)	0.1479	0.1161	0.0556

**Fig. 2** The molecular structure of **1c**. Thermal ellipsoids are drawn at 30% probability level. Mo(1)–Mo(2) separation is 2.6060(4) Å.

pyridinium cations and anionic clusters. The ORTEP drawing of **1c** is shown in Fig. 2, whilst selected bond lengths are given in Table 3. The same atom numbering scheme pertains to all three compounds. The tetranuclear dianion is located on a crystallographic centre of symmetry, with the unique molybdenum atoms, Mo(1) and Mo(2), displaying two distinct [MoO₅X] coordination environments. Both metal atoms have in common a terminal, multiply bonded oxo group, a terminal halide, a

μ -bridging oxygen [O(3)], a triply-bridging oxygen [O(4)], and a doubly-bridging alkoxide oxygen [O(5)]. Whilst the sixth coordination site of Mo(1) is occupied with another triply bridging ligand, the symmetry equivalent of O(4), that of Mo(2) is another terminal position and is occupied by an alcohol ligand. The highly distorted octahedral environment about the metal centres results from the weak axial interactions *trans* to the multiply bonded terminal oxo groups. The ten independent Mo–O bond lengths cover a wide range [\approx 1.67–2.29 Å]; the differences are understandable in terms of different types and orders of the bonds. The Mo(v) atoms show bonding characteristics similar to other {Mo₂O₄}²⁺ compounds which have been structurally characterized:^{2a} a bent Mo₂O₂ bridge and a short distance between Mo(1) and Mo(2), 2.6005(4) Å in **1a**, 2.6083(5) Å in **1b**, and 2.6060(4) Å in **1c**, which implies bonding overlap between two d orbitals of molybdenum atoms. Other Mo–Mo distances within the Mo₄ rhombus represent non-bonding Mo...Mo interactions (Table 4). The cluster may be viewed in its polyhedral representation as the assembly of four octahedra, with two sharing edges with all three neighbours, and the other two having common edges with two adjacent octahedra only.

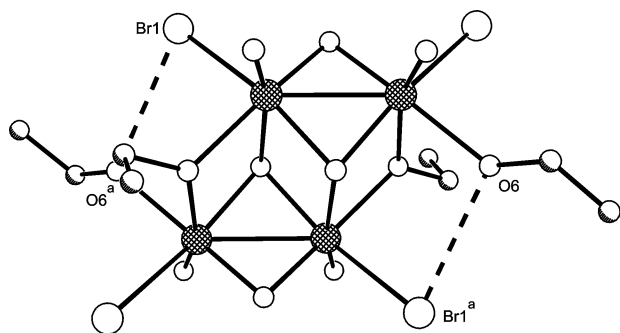
The terminal oxygen donor ligand on Mo(2) has been identified as an alcohol. The crystallographic identification of alcohol as the terminal ligand on Mo(2) is corroborated by the infrared data (*vide infra*). The distances are comparable to other molybdenum(v) compounds containing terminally bound

Table 3 Relevant structural parameters (Å) for **1a**, **1b** and **1c**

	1a	1b	1c
Mo–Mo ^a	2.6005(4)	2.6083(5)	2.6060(4)
Mo–O _t ^b	1.678(2)	1.6701(18)	1.672(2)
	1.682(2)	1.6805(17)	1.678(2)
Mo–O(μ) ^c	1.946(2)	1.9479(17)	1.946(2)
	1.936(2)	1.9407(17)	1.934(2)
Mo–O(μ ₃)	1.980(2)–2.269(2)	1.9789(16)–2.2982(16)	1.977(2)–2.290(2)
Mo–OR(μ) ^d	2.110(2)	2.0993(16)	2.104(2)
	2.176(2)	2.1731(17)	2.173(2)
Mo–ROH ^e	2.2070(23)	2.2025(19)	2.2007(22)
Mo(1)–X(1) ^f	2.4502(8)	2.4506(7)	2.5902(4)
Mo(2)–X(2) ^f	2.4166(8)	2.4203(8)	2.5722(4)

^a Mo(1)–Mo(2) distance. ^b Mo(1)–O(1) and Mo(2)–O(2) distances. ^c Mo(1)–O(3) and Mo(2)–O(3) distances. ^d Mo(1)–O(5) and Mo(2)–O(5) distances where O(5) is a μ-bridging alkoxide oxygen. ^e Mo(2)–O(6) where O(6) is a terminal alcohol oxygen. ^f X = Cl for **1a** and **1b**; X = Br for **1c**.

alcohols *i.e.* 2.264(3) Å for methanol in [Mo₄O₄(μ-O)₄(μ-OMe)₂(MeOH)₂(HB(pz)₃)₂] (HB(pz)₃[−] = hydrotripyrzolyborate)¹⁸ and 2.144(4) Å for ethanol in [Mo₄O₆(OEt)₄(HOEt)₂Cl₄].¹⁹ The coordinated alcohol is involved in a relatively strong intramolecular hydrogen bond with one of the coordinated halides (Fig. 3, Table 5).²⁰ The same kind of interaction occurs in the

**Fig. 3** Intramolecular hydrogen bond between ethanol oxygen O(6) and bromide Br(1) in **1c**.

related compounds [Mo₄O₆(OEt)₄(HOEt)₂Cl₄]¹⁹ (3.038 Å) and [Mo₄O₆(OⁿPr)₄(HOⁿPr)₂Cl₄]²¹ (2.998 Å). The hydrogen bonding interaction influences the variations in the molybdenum-to-halide bonds (see Table 3); the halide involved in the hydrogen bond binds to molybdenum at a longer distance. On the whole, the molybdenum-to-chlorine bonds are within normal range when compared to the literature data.^{5,6,19,21} The molybdenum-to-bromine distances are also consistent with those reported for (PyH)[MoOBr₄(H₂O)]·2/3PyHBr [2.498(4)–2.563(4) Å]²² and [Mo₂(OⁿPr)₆Br₄]²³ [2.579(1)–2.584(1) Å].²³

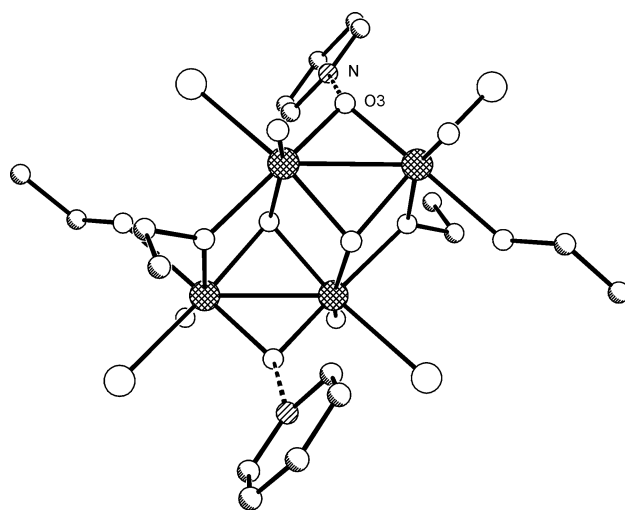
The pyridinium cations and the anionic clusters are linked through the agency of hydrogen bonds of moderate strength, localized between the pyridinium nitrogen and the doubly-bridging oxygen from the anion, N···O(3) = 2.759(5) Å in **1a**, 2.690(4) Å in **1b**, and 2.697(4) Å in **1c** (Fig. 4). A similar bonding pattern was observed in [C₁₆H₁₃N₂S₂]₂[Mo₄O₈(OEt)₂(HOEt)₂Cl₄]²⁴ where the organic cations are linked to the anions through the N···O bridges with an even shorter distance of 2.65 Å.

Two compounds containing the same tetranuclear anions, but with different cations, [C₁₆H₁₃N₂S₂]₂[Mo₄O₈(OEt)₂(HOEt)₂Cl₄]²⁴ and [Et₃NH]₂[Mo₄O₈(OMe)₂(HOMe)₂Cl₄]²⁵ have been described previously. As the earlier crystallographic studies failed to locate the alcoholic protons, initially mixed valence character was proposed for both. The need to reformulate these complexes was recognized by Lincoln and Koch.¹⁸ With one molybdenum atom from the pair having oxidation state +5, and the other +6, the Mo–Mo bonds should be slightly longer, which was not the case. The Mo–O bonds of the terminally coordinated ligand (≈2.1 Å) which were outside the range for

Table 4 The Mo···Mo contacts (Å) within the Mo₄ rhombus in **1a**, **1b**, **1c**, **2a** and **2b**

	Mo(1)–Mo(1) ^a	Mo(1)–Mo(2) ^a	Mo(2)–Mo(2) ^a
1a	3.3838(6)	3.4460(4)	5.0818(6)
1b	3.4271(8)	3.4463(4)	5.0613(7)
1c	3.4150(5)	3.4462(4)	5.0669(5)
2a ^b	3.2908(10)	3.4426(7)	5.1168(10)
	3.2600(9)	3.4452(7)	5.1476(11)
2b ^b	3.2834(8)	3.4473(6)	5.1300(8)
	3.2489(7)	3.4418(5)	5.1596(8)

^a Symmetry equivalent. ^b The Mo···Mo contacts in the first molecule are written on the first row, and for the second on the second row.

**Fig. 4** The pyridinium cation···anionic cluster interaction in **1c**.

the terminal alkoxides (1.81–1.98 Å),²⁷ also suggested these to be terminally bound alcohols.

The crystal structures of [Mo₄O₈(OEt)₂Br₂Py₄] and [Mo₄O₈(OEt)₂Br₂Py₄]·2CH₃CN, **2a and **2b**.** The asymmetric units of **2a** and **2b** contain two halves of the neutral cluster molecules showing minor differences in the orientation of pyridine rings and ethyl carbon atoms. There are no significant differences in the core dimensions of the two independent molecules. **2b** also contains acetonitrile solvent of crystallization. The ORTEP drawing of **2a** is shown in Fig. 5, whilst selected bond lengths are given in Tables 4, 6 and 7. The four Mo(v) d¹ electrons in each molecule pair to produce two metal–metal bonds [Mo(1)–Mo(2) = 2.5795(7) Å, Mo(3)–Mo(4) = 2.5872(7) Å in **2a**, and Mo(1)–Mo(2) = 2.5817(6) Å, Mo(3)–Mo(4) = 2.5966(5) Å in **2b**]. The molecules are packed together with normal van der Waals' forces. The structure of [Mo₄O₈(OEt)₂Br₂Py₄] finds

Table 5 The alcohol...halide intramolecular interaction (Å)

Compound	O(6) ... X(1)	Ref.
1a	3.075(3)	This work
1b	3.063(2)	This work
1c	3.180(3)	This work
[Et ₃ NH] ₂ [Mo ₄ O ₈ (OMe) ₂ -(HOMe) ₂ Cl ₄] ^a	3.056	25
[C ₁₆ H ₁₃ N ₂ S ₂] ₂ [Mo ₄ O ₈ (OEt) ₂ -(HOEt) ₂ Cl ₄] ^a	3.078	24

^a The O...X contacts were taken from the CCDC.²⁶

Table 6 Selected bond lengths (Å) for **2a**^a

Mo(1)–Mo(2)	2.5795(7)	Mo(3)–Mo(4)	2.5872(7)
Mo(1)–O(1)	1.682(5)	Mo(3)–O(3)	1.679(4)
Mo(1)–O(5)	2.107(4)	Mo(3)–O(9)	2.121(4)
Mo(1)–O(6)	1.924(4)	Mo(3)–O(8)	1.924(4)
Mo(1)–O(7)	1.983(4)	Mo(3)–O(10)	1.997(4)
Mo(1)–O(7) ^b	2.243(4)	Mo(3)–O(10) ^c	2.206(4)
Mo(1)–N(1)	2.232(5)	Mo(3)–N(3)	2.222(5)
Mo(2)–O(2)	1.686(5)	Mo(4)–O(4)	1.684(5)
Mo(2)–O(5) ^b	2.218(4)	Mo(4)–O(9) ^c	2.197(4)
Mo(2)–O(6)	1.935(4)	Mo(4)–O(8)	1.941(4)
Mo(2)–O(7)	1.998(4)	Mo(4)–O(10)	2.008(4)
Mo(2)–Br(2)	2.5355(11)	Mo(4)–Br(4)	2.5747(10)
Mo(2)–N(2)	2.267(5)	Mo(4)–N(4)	2.271(5)

^a The atom labelling scheme for the second molecule is not presented, nevertheless the corresponding bonds are given in the third and fourth columns. ^b Related through symmetry operation: $-x - 2, -y - 1, 2 - z$. ^c Related through symmetry operation: $-x - 1, -y, 2 - z$.

Table 7 Selected bond lengths (Å) for **2b**^a

Mo(1)–Mo(2)	2.5817(6)	Mo(3)–Mo(4)	2.5966(5)
Mo(1)–O(1)	1.682(3)	Mo(3)–O(3)	1.676(3)
Mo(1)–O(5)	2.112(3)	Mo(3)–O(9)	2.116(3)
Mo(1)–O(6)	1.928(4)	Mo(3)–O(8)	1.930(3)
Mo(1)–O(7)	1.990(3)	Mo(3)–O(10)	1.987(3)
Mo(1)–O(7) ^b	2.243(3)	Mo(3)–O(10) ^c	2.213(3)
Mo(1)–N(1)	2.209(4)	Mo(3)–N(3)	2.216(4)
Mo(2)–O(2)	1.680(4)	Mo(4)–O(4)	1.683(3)
Mo(2)–O(5) ^b	2.219(3)	Mo(4)–O(9) ^c	2.201(3)
Mo(2)–O(6)	1.929(3)	Mo(4)–O(8)	1.939(3)
Mo(2)–O(7)	2.000(3)	Mo(4)–O(10)	2.012(3)
Mo(2)–Br(2)	2.5553(7)	Mo(4)–Br(4)	2.5464(7)
Mo(2)–N(2)	2.279(4)	Mo(4)–N(4)	2.296(4)

^a Same atom labelling scheme is applied as for **2a**. ^b Related through symmetry operation: $-x, 1 - y, 2 - z$. ^c Related through symmetry operation: $-x - 1, 1 - y, 3 - z$.

one closely related analogue, namely [Mo₄O₈(OMe)₂Cl₂Py₄]⁶ with bridging methoxides and terminal chlorides, in place of ethoxides and bromides, respectively.

More general considerations

The centrosymmetric core structure of **1a**, **1b**, **1c**, **2a** and **2b** may be envisioned as a very compact fusion of two {Mo₂O₄}²⁺ units (Fig. 6a): the originally doubly-bridging oxygen from the first dimer coordinates to the metal from the second dimer and thus becomes a triply-bridging ligand. Similarly, a doubly-bridging oxygen from the second dimer attaches to the first dimer. The dimers are held together also through two doubly-bridging alkoxides. The six peripheral positions of the metal oxide core, {Mo₄O₄(μ₃-O)₂(μ-O)₂(μ-OR)₂}²⁺, are distributed among four halides and two alcohols in **1a**, **1b** and **1c**, or two bromides and four pyridines in **2a** and **2b**. Several compounds containing this same core structure have been structurally characterized, with overall cluster charge dependent upon the nature of the terminal ligands *i.e.* [Mo₄O₈(OⁱPr)₄Py₄]²⁸ [Mo₄O₈(OMe)₄(4-MePy)₄] (4-MePy = 4-methylpyridine), [Mo₄O₈

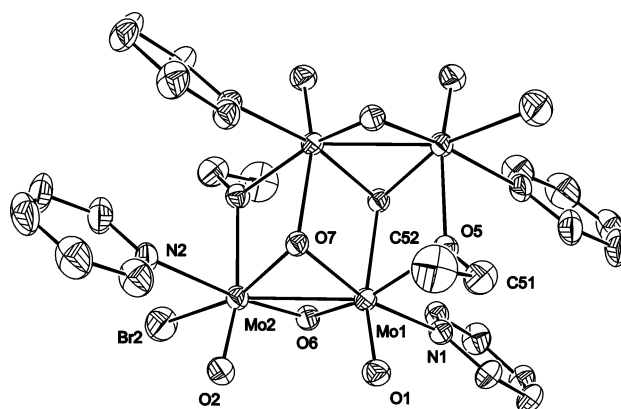


Fig. 5 The molecular structure of [Mo₄O₈(OEt)₂Br₂Py₄] **2a**. One independent molecule is shown only.

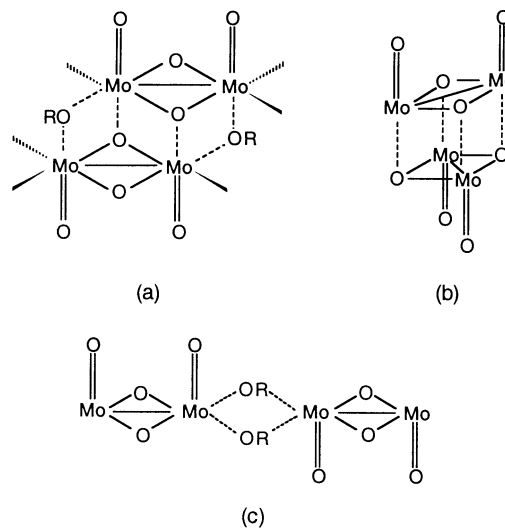


Fig. 6 Schematic representation of core structures obtained upon different arrangements of two building blocks: (a) {Mo₄O₄(μ₃-O)₂(μ-O)₂(μ-OR)₂}²⁺, (b) cube-like {Mo₄O₄(μ₃-O)₄}⁴⁺ and (c) linear {Mo₄O₄(μ-O)₄(μ-OR)₂}²⁺.

(OMe)₂Cl₂Py₄]⁶ [Mo₄O₈(OMe)₂(MoO₄)₂(HMoO₄)₂]⁴⁻,²⁹ and [Mo₄O₈(OMe)₂(C₄O₄)₂(HC₄O₄)₂]⁴⁻.³⁰ Their structures support Bradley's theory for metal alkoxides that the metal atoms achieve their preferred coordination by the minimum degree of oligomerization.³¹ Two more variants of this core structure are known, one without the bridging alkoxides, {Mo₄O₄(μ₃-O)₂(μ-O)₂}⁴⁺, found in molybdoarsenates³² and another, {Mo₄O₄(μ₃-O)₂(μ-OR)₄}⁴⁺, built of related {Mo₂O₂(μ-O)(μ-OR)}³⁺ dimers.^{5,19,21} As witnessed by numerous examples, this type of tetranuclear core represents a persistent chemical unit.

Two {Mo₂O₄}²⁺ moieties may associate in two more ways to give (a) another very compact, cube-like {Mo₄O₄(μ₃-O)₄}⁴⁺ core with a tetrahedral arrangement of molybdenum atoms and (b) an open, chain-like {Mo₄O₄(μ-O)₄(μ-OR)₂}²⁺ (Fig. 6b and c). The main differences in the three core structures lie in the number of triply-bridging oxo groups. The cubane structure finds examples mostly among polymeric phosphomolybdates³³ and only two molecular compounds, [Mo₄O₈(Me₂POS)₄]³⁴ and [Mo₄O₈(OSiMe₃)₄(HNMe₂)₄]³⁵. An open, chain-like structure is even less common. The only examples are [Mo₄O₄(μ-O)₄(μ-OMe)₂(MeOH)₂(HB(pz)₃)₂]¹⁸ and [Mo₆O₁₀(OⁱPr)₁₂]³⁶.

The crystal structure of [LH₂][Mo₆O₁₉]·L·2EtOH **3.** The X-ray structural analysis revealed the structure of **3** (Fig. 7) to be composed of polymeric organic cations and well-known Lindquist anions, [Mo₆O₁₉]²⁻.³⁷ Hexamolybdate(vi), [Mo₆O₁₉]²⁻, is made up of six octahedra, arranged in a compact edge-sharing mode. Each octahedron shares four of its edges

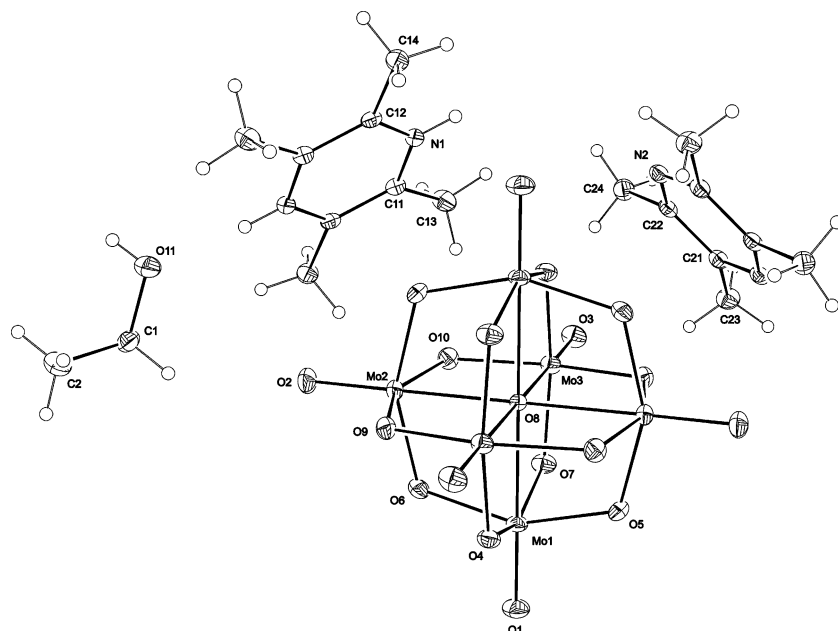


Fig. 7 The molecular structure of **3** with the atom labelling scheme.

Table 8 Selected bond lengths (Å) within $[\text{Mo}_6\text{O}_{19}]^{2-}$ in **3**

Mo(1)–O(1)	1.6828(18)	Mo(1)–O(8)	2.32238(19)
Mo(2)–O(2)	1.6826(18)	Mo(2)–O(8)	2.3143(2)
Mo(3)–O(3)	1.6837(17)	Mo(3)–O(8)	2.3224(2)
Mo(1)–O(4)	1.8773(17)	Mo(1)–O(6)	1.9353(18)
O(4)–Mo(3) ^a	1.9868(17)	O(6)–Mo(2)	1.9266(17)
Mo(1)–O(7)	1.9725(17)	Mo(2)–O(9)	1.9237(17)
O(7)–Mo(3)	1.8730(17)	O(9)–Mo(3) ^a	1.9314(17)
Mo(1)–O(5)	1.9217(18)	Mo(2)–O(10)	1.9253(17)
O(5)–Mo(2) ^a	1.9323(18)	O(10)–Mo(3)	1.9242(17)

^a Related through symmetry operation: $2 - x, -y, -z$.

with four adjacent octahedra. Selected bond lengths for $[\text{Mo}_6\text{O}_{19}]^{2-}$ are given in Table 8.

The oxygen atoms fall into three non-equivalent classes: there are six terminal oxygens (O_t), twelve μ -bridging oxygens (O_b), and a central oxygen (O_c) which adopts a μ_6 -bridging mode. The Mo–O bonds also fall into three classes, terminal Mo–O bonds [1.6826(18)–1.6837(17) Å], bridging Mo– O_b bonds [1.8730(17)–1.9868(17) Å], and central Mo– O_c bonds [2.3143(2)–2.3224(2) Å]. The Mo– O_b distances display significant variations. Within the Mo(1)–Mo(3)–Mo(1)ⁱ–Mo(3)ⁱ [(i) symmetry equivalent: $2 - x, -y, -z$] equatorial belt of the cluster, a pattern of bond length alternation is evident: each O_b [O(4), O(7) or their symmetry equivalents] forms one short [1.8730(17), 1.8773(17) Å] and one long [1.9725(17), 1.9868(17) Å] bond to its adjacent Mo atoms. No such alternation is observed within other Mo– O_b distances. These differences can only be ascribed to the packing influences of the anion with the cations. Comparison of the structural parameters with the cyclophosphazene complex, $[\text{HN}_3\text{P}_3(\text{NMe}_2)_6]_2[\text{Mo}_6\text{O}_{19}]$,³⁸ shows an alternation of long and short Mo– O_b distances in all three $\text{Mo}_4(\text{O}_b)_4$ rings. Each Mo atom is displaced from the centre of the MoO_6 octahedron towards the terminal oxygen, giving rise to long Mo– O_c bonds. In spite of distortions, the symmetry of the anion approximates O_h .

The ethanol molecule of crystallization forms two types of hydrogen bonds: type **a** with the neutral base $[\text{O}(11) \cdots \text{N}(2) = 2.767(3)$ Å] where the ethanol oxygen acts as a donor of the hydrogen bond and type **b** with a doubly protonated tetramethylpyrazine $[\text{N}(1) \cdots \text{O}(11) = 2.785(3)$ Å] where it is an acceptor (Fig. 8a). Through the propagation of the relatively strong interactions between the cations, ethanol and neutral base molecules infinite, zig-zag chains are formed; their packing

being such as to create a grid-like structure with channels running parallel to the x -axis. The orientation of the aromatic rings along the chain segments [the planes of L and LH_2^{2+} rings are rotated by $71.76(11)^\circ$ with respect to each other] is such to define cavities that accommodate anionic clusters (Fig. 8b and c).

$[\text{Mo}_6\text{O}_{19}]^{2-}$ appears as a counter ion in scores of compounds, for instance in organic–inorganic conducting materials such as $(\text{TTF})_2[\text{Mo}_6\text{O}_{19}]$ and $(\text{TTF})_3[\text{Mo}_6\text{O}_{19}]$ (TTF = tetrathiafulvalene)³⁹ where the planar cation acts as a π -donor and hexamolybdate(vi) as an electron acceptor. In $[\{\text{Fe}(\text{tpypr})\}_3\text{Fe}(\text{Mo}_6\text{O}_{19})_2] \cdot x\text{H}_2\text{O}$ (tpypr = tetrapyrrolylporphyrin), a novel molybdenum oxide-based composite material, the $[\text{Mo}_6\text{O}_{19}]^{2-}$ clusters entrained into a three-dimensional framework $[\text{Fe}_4(\text{tpypr})_3]_n^{4n+}$ adopt a charge-compensating and space-filling role.⁴⁰ In broader terms the structure of the latter resembles that of **3**.

Vibrational spectroscopy

The spectra of $(\text{PyH})_2[\text{Mo}_4\text{O}_8(\text{OR})_2(\text{HOR})_2\text{X}_4]$ **1a**, **1b** and **1c** show very similar gross features; in all two sharp bands occur in the Mo=O stretching region, at 966 and 946 cm^{-1} for **1a**, 969 and 946 cm^{-1} for **1b**, and at 968 and 946 cm^{-1} for **1c**. The O–H stretch of the hydrogen bonded alcohol occurs at 3223 cm^{-1} for **1a**, 3217 cm^{-1} for **1b** and 3218 cm^{-1} for **1c**; the shift to a lower frequency region is in accordance with the involvement of alcohol in hydrogen bonds.⁴¹ In $[\text{Mo}_4\text{O}_6(\text{OEt})_4(\text{HOEt})_2\text{Cl}_4]$, where ethanol is also engaged in an intramolecular bonding interaction with chloride, the O–H stretching vibration occurs at 3210 cm^{-1} .¹⁹ C–H stretches of the alkyl groups appear at 2950, 2932 and 2831 cm^{-1} in **1a**, 2980, 2930 and 2888 cm^{-1} in **1b**, and 2980, 2928 and 2887 cm^{-1} in **1c**. The positions of bands in **1b** and **1c** are consistent with the reported spectral data for $[\text{C}_{16}\text{H}_{13}\text{N}_2\text{S}_2]_2[\text{Mo}_4\text{O}_8(\text{OEt})_2(\text{HOEt})_2\text{Cl}_4]$ (2950, 2920 and 2700 cm^{-1}).²⁴

The IR spectrum of **2a** displays a complex pattern of features between 1650 and 400 cm^{-1} that are associated with the presence of coordinated pyridine; it shows a pronounced similarity with the spectrum of related $[\text{Mo}_4\text{O}_8(\text{OMe})_2\text{Cl}_2\text{Py}_4]$.⁶ Compound **2a** exhibits two Mo=O stretches at 963 and 942 cm^{-1} for two distinct types of Mo=O. A weak absorption at 2850 cm^{-1} may be attributed to ethoxide C–H stretching vibrations.

In the IR spectrum of **3**, the Mo=O stretching vibration occurs at 957 cm^{-1} , strong bands are observed at 799, 601 and 431 cm^{-1} ; this pattern is characteristic for hexamolybdate(vi)

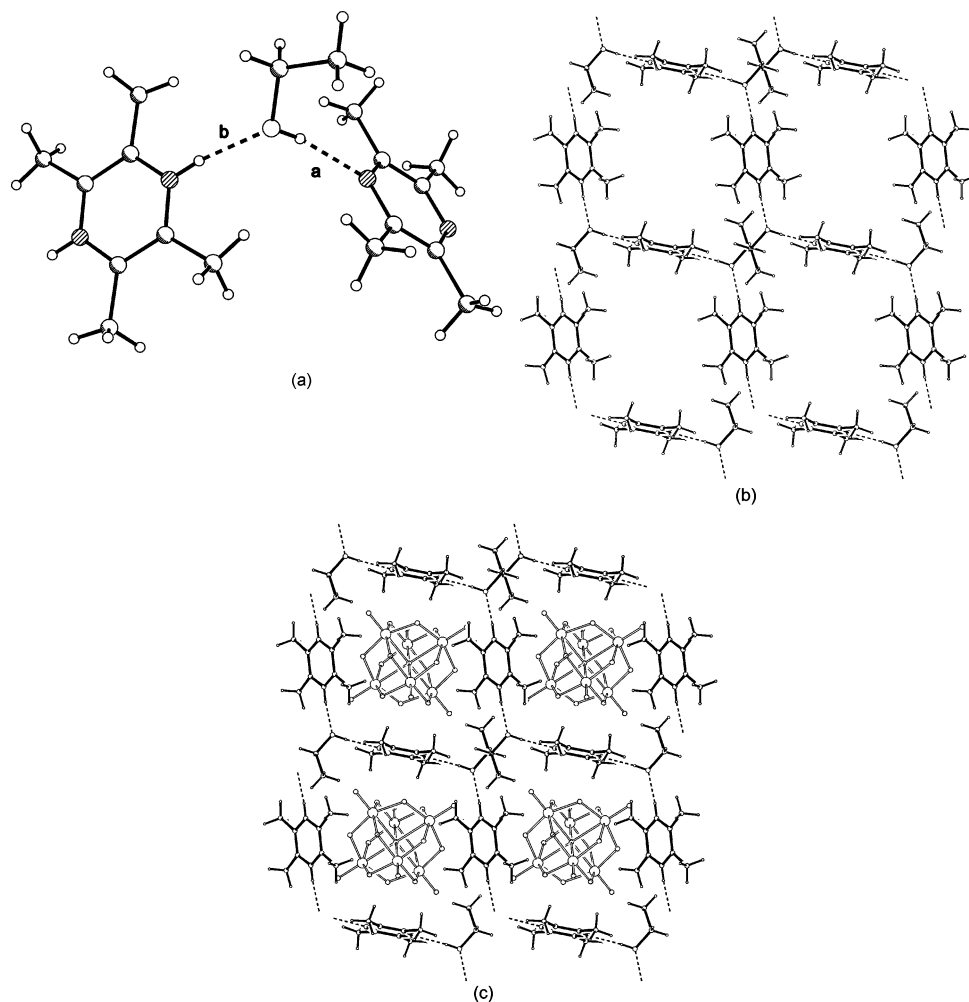


Fig. 8 (a) Hydrogen bonds between ethanol and tetramethylpyrazine (a), and ethanol and doubly protonated tetramethylpyrazine (b). (b) Infinite chains in **3** viewed along the *x*-axis. (c) The organic network with entrained anionic clusters.

species.⁴² The absorption at 1644 cm^{-1} confirms the presence of fully protonated tetramethylpyrazine and a weak absorption at 3162 cm^{-1} the hydrogen bonded ethanol molecules. The intensity of the latter band rapidly diminishes with time.

Conclusions

The anionic $[\text{Mo}_4\text{O}_8(\text{OR})_2(\text{HOR})_2\text{X}_4]^{2-}$ clusters are additions to the series of oxomolybdenum(v) clusters obtained from the mononuclear oxohalomolybdates(v). In alcoholic solutions of pyridines (R-Py), $(\text{PyH})_2[\text{MoOCl}_5]$ has been known to readily generate reactive $\{\text{Mo}_2\text{O}_4\}^{2+}$ fragments which attain stability through further aggregation.^{6,43} Stable oligomers *i.e.* $[\text{Mo}_4\text{O}_8(\text{OMe})_2\text{Cl}_2(\text{R-Py})_4]$, $[\text{Mo}_6\text{O}_{12}(\text{OMe})_6(\text{R-Py})_4]$, $[\text{Mo}_8\text{O}_{16}(\text{OMe})_8(\text{R-Py})_4]$ and $[\text{Mo}_{12}\text{O}_{28}(\text{OEt})_4(\text{R-Py})_8]$, were obtained with the assembly of two, three, four and six building blocks, respectively. The octanuclear $[\text{Mo}_8\text{O}_{16}(\text{OMe})_8(\text{R-Py})_4]$ presents an unusual manifestation of structural isomerism as the same building blocks were seen to form two distinct architectures.^{43c} A third arrangement of four $\{\text{Mo}_2\text{O}_4\}^{2+}$ units was observed in $[\text{Mo}^{\text{V}}_8\text{Mo}^{\text{VI}}_2\text{O}_{26}(\text{R-Py})_8]$.^{43b} It is pertinent to mention here another reaction system that has produced a series of related oxoethoxymolybdenum(v) clusters.

$[\text{Mo}_2\text{O}_2(\mu\text{-OEt})_2(\mu\text{-HOEt})\text{Cl}_4]$,⁴⁴ the first unambiguously characterized product of the reaction between MoCl_5 and ethanol, possesses a highly labile site, a doubly-bridging ethanol. Its chemistry has been thoroughly explored and it was shown to produce clusters built of related $\{\text{Mo}_2\text{O}_2(\mu\text{-O})(\mu\text{-OEt})\}^{3+}$ moieties.^{5,19,45} The reasons for the ready formation of the oligonuclear polyoxoalkoxymolybdates(v) are two-fold.

Firstly, the dimerisation through MoO_2Mo bridging systems with the concomitant interaction between two d^1 ions is a highly favoured process³⁷ and secondly, the ability of the alkoxides to adopt μ - and μ_3 -bridging roles, makes them perfect ligands in further condensation reactions.

The anticipated role of an N,N-bidentate tetramethylpyrazine to act as a connector between $\{\text{Mo}_2\text{O}_4\}^{2+}$ units was not realized, rather it functions as a structure directing agent whose presence is prerequisite for the isolation of $(\text{PyH})_2[\text{Mo}_4\text{O}_8(\text{OR})_2(\text{HOR})_2\text{X}_4]$. The use of pyrazine instead fails to give the same crystalline phase. The observed effect is hardly without precedents. Not only N-containing organic molecules, but also inorganic salts have been seen to exert a crucial effect over the architecture of the metal cluster or oxide, an approach that has been widely used in inorganic crystal engineering.^{11a,46} Nevertheless, tetramethylpyrazine could have assumed two other structural roles: (a) in its protonated form as a counter ion or as such a participant in the extensive network of hydrogen bonding as demonstrated with **3** and (b) as a monodentate ligand capping the ends of the oligomer and thus precluding a more extended structure. It is of interest to compare the reaction conditions employed in the syntheses of $(\text{PyH})_2[\text{Mo}_4\text{O}_8(\text{OEt})_2(\text{HOEt})_2\text{Br}_4]$ **1c**, specifically Procedure a *vs.* Procedure b. The nitrogen donor ligand used in Procedure a is tetramethylpyrazine, while in Procedure b it is a monodentate pyridine. When the amounts of nitrogen ligands are relatively small, an oxygen-donor ligand, alcohol, is chosen rather than a nitrogen ligand, and the isolated product is $(\text{PyH})_2[\text{Mo}_4\text{O}_8(\text{OEt})_2(\text{HOEt})_2\text{Br}_4]$. With the increased amounts of nitrogen donor ligands (*vide supra* the preparation of **2a** and **2b**), the

nitrogen ligand coordinates to the metal and the product obtained is $[\text{Mo}_4\text{O}_8(\text{OEt})_2\text{Br}_2\text{Py}_4]$. Attempts to coordinate tetramethylpyrazine to molybdenum also by increasing the amounts of the ligand, have not been met with success as yet.

The formation of $[\text{LH}_2][\text{Mo}_6\text{O}_{19}]\cdot\text{L}\cdot 2\text{EtOH}$ **3** is not easy to rationalize. However, it is evident that small amounts of water present in ethanol are of key importance in the oxidation of molybdenum(v) species to molybdenum(vi). Although hydrogen bonding endows stability to the coordinated alcohol in the solid state, the peripheral ligands in $(\text{PyH})_2[\text{Mo}_4\text{O}_8(\text{OR})_2(\text{HOR})_2\text{X}_4]$, the alcohol and the halides, are labile and can be easily displaced under appropriate conditions. In view of our previous studies, the alcoholic solvents containing traces of water certainly provide an environment that promotes further substitution and oxidation reactions.⁴³

In conclusion, this work illustrates a subtle reaction system which reproducibly generates oxoalkoxymolybdenum(v) halide complexes *via* substitution and polymerization reactions of simple molybdenum(v) starting materials. Studies to discern the generality of this procedure with other alcohols are under way.

Acknowledgements

We are grateful to the Slovenian Ministry of Science and Education for supporting this work through research grant JI-1460-0103-99. We also thank the same agency for funds to purchase the Nonius Kappa CCD diffractometer. The work at Syracuse University was supported by a grant from the National Science Foundation, CHE9987471.

References

- (a) C. L. Hill (Guest editor), *Chem. Rev.*, 1998, **98**, 1–390; (b) W. G. Klemperer, T. A. Marquart and O. M. Yaghi, *Angew. Chem., Int. Ed. Engl.*, 1992, **31**, 49.
- (a) H. K. Chae, W. G. Klemperer and T. A. Marquart, *Coord. Chem. Rev.*, 1993, **128**, 209; (b) Q. Chen and J. Zubieta, *Coord. Chem. Rev.*, 1992, **114**, 107; (c) M. I. Khan and J. Zubieta, *Prog. Inorg. Chem.*, 1995, **43**, 1.
- H. K. Chae, W. G. Klemperer, D. E. Paez Loyo, V. W. Day and T. A. Eberspacher, *Inorg. Chem.*, 1992, **31**, 3187.
- J. D. McKinney, H. Chen, T. A. Hamor, K. Paxton and C. J. Jones, *J. Chem. Soc., Dalton Trans.*, 1998, 2163.
- C. Limberg, M. Büchner, K. Heinze and O. Walter, *Inorg. Chem.*, 1997, **36**, 872.
- B. Modéc, J. V. Brenčič, L. Golič and G. Giester, *Inorg. Chim. Acta*, 2000, **307**, 32.
- D. J. Darensbourg, R. L. Gray and T. Delord, *Inorg. Chim. Acta*, 1985, **98**, L39.
- M. I. Khan, A. Müller, S. Dillinger, H. Bögge, Q. Chen and J. Zubieta, *Angew. Chem., Int. Ed. Engl.*, 1993, **32**, 1780.
- J.-H. Chou, J. A. Hanko and M. G. Kanatzidis, *Inorg. Chem.*, 1997, **36**, 4.
- (a) S. Kitagawa, M. Munakata and T. Tanimura, *Inorg. Chem.*, 1992, **31**, 1714; (b) N. S. Persky, J. M. Chow, K. A. Poschmann, N. N. Lacuesta, S. L. Stoll, S. G. Bott and S. Obrey, *Inorg. Chem.*, 2001, **40**, 29; (c) C. Näther and I. Jeß, *Acta Crystallogr., Sect. C*, 2001, **57**, 260.
- (a) Y. Xu, J. Lu and N. K. Goh, *J. Mater. Chem.*, 1999, **9**, 1599; (b) M. Hong, R. Cao, D. Sun and J. Weng, *Acta Crystallogr., Sect. E*, 2001, **57**, m159.
- (a) G. R. Hanson, A. A. Brunette, A. C. McDonell, K. S. Murray and A. G. Wedd, *J. Am. Chem. Soc.*, 1981, **103**, 1953; (b) H. K. Saha and A. K. Banerjee, *Inorg. Synth.*, 1974, **15**, 100.
- G. M. Sheldrick, SADABS, A Program for Absorption Correction with the Siemens SMART Area-Detector system, University of Göttingen, 1996.
- A. C. T. North, D. C. Phillips and F. S. Mathews, *Acta Crystallogr., Sect. A*, 1968, **24**, 351.
- G. M. Sheldrick, SHELXS 97 and SHELXL 97, Programs for Crystal Structure Solution and Refinement, University of Göttingen, 1997.
- SHELXTL version 5.03, Software Package for Crystal Structure Determination, Siemens Analytical X-ray Instrument Division, Madison, WI, 1994.
- A. L. Spek, *Acta Crystallogr. Sect. A*, 1990, **46**, C34.
- (a) S. A. Koch and S. Lincoln, *Inorg. Chem.*, 1982, **21**, 2904; (b) S. Lincoln and S. A. Koch, *Inorg. Chem.*, 1986, **25**, 1594.
- C. Limberg, A. J. Downs, A. J. Blake and S. Parsons, *Inorg. Chem.*, 1996, **35**, 4439.
- The sums of the corresponding van der Waals radii are 3.27 Å for O + Cl and 3.37 Å for O + Br. Data were taken from B. Douglas, D. McDaniel and J. Alexander, *Concepts and Models of Inorganic Chemistry*, John Wiley & Sons, Inc., New York, 3rd edn., 1994, p. 102.
- J. A. Beaver and M. G. B. Drew, *J. Chem. Soc., Dalton Trans.*, 1973, 1376.
- A. Bino and F. A. Cotton, *Inorg. Chem.*, 1979, **18**, 2710.
- M. H. Chisholm, C. C. Kirkpatrick and J. C. Huffman, *Inorg. Chem.*, 1981, **20**, 871.
- M. F. Belicchi, G. G. Fava and C. Pelizzi, *J. Chem. Soc., Dalton Trans.*, 1983, 65.
- H. Kang, S. Liu, S. N. Shaikh, T. Nicholson and J. Zubieta, *Inorg. Chem.*, 1989, **28**, 920.
- F. H. Allen, O. Kennard and R. Taylor, *Acc. Chem. Res.*, 1983, **16**, 146.
- M. H. Chisholm, *Polyhedron*, 1983, **2**, 681.
- M. H. Chisholm, J. C. Huffman, C. C. Kirkpatrick, J. Leonelli and K. Folting, *J. Am. Chem. Soc.*, 1981, **103**, 6093.
- S. Liu and J. Zubieta, *Polyhedron*, 1989, **8**, 537.
- Q. Chen, S. Liu and J. Zubieta, *Inorg. Chim. Acta*, 1989, **164**, 115.
- D. C. Bradley, *Nature (London)*, 1958, **182**, 1211.
- (a) E. Dumas, C. Livage, D. Riou and G. Herve, *Eur. J. Solid State Inorg. Chem.*, 1997, 151; (b) M. I. Khan, Q. Chen and J. Zubieta, *J. Chem. Soc., Chem. Commun.*, 1993, 356; (c) Q. He and E. Wang, *Inorg. Chim. Acta*, 2000, **298**, 235.
- (a) L. A. Mundi and R. C. Haushalter, *J. Am. Chem. Soc.*, 1991, **113**, 6340; (b) E. W. Corcoran, Jr., *Inorg. Chem.*, 1990, **29**, 157; (c) R. C. Haushalter, K. G. Strohmaier and F. W. Lai, *Science*, 1989, **246**, 1289.
- R. Mattes and K. Mühlisepfen, *Z. Naturforsch., Teil B*, 1980, **35**, 265.
- S. G. Kim, D. A. Keszler and C. W. DeKock, *Inorg. Chem.*, 1991, **30**, 574.
- M. H. Chisholm, K. Folting, J. C. Huffman and C. C. Kirkpatrick, *Inorg. Chem.*, 1984, **23**, 1021.
- M. T. Pope, *Prog. Inorg. Chem.*, 1991, **39**, 181.
- (a) H. R. Allcock, E. C. Bissell and E. T. Shawl, *Inorg. Chem.*, 1973, **12**, 2963; (b) T. M. Che, V. W. Day, L. C. Francesconi, M. F. Fredrich, W. G. Klemperer and W. Shum, *Inorg. Chem.*, 1985, **24**, 4055.
- (a) S. Triki, L. Quahab, J. Padiou and D. Grandjean, *J. Chem. Soc., Chem. Commun.*, 1989, 1068; (b) E. Coronado and C. J. Gomez-Garcia, *Chem. Rev.*, 1998, **98**, 273.
- D. Hagrman, P. J. Hagrman and J. Zubieta, *Angew. Chem., Int. Ed.*, 1999, **38**, 3165.
- N. B. Colthup, L. H. Daly and S. E. Wiberley, *Introduction to Infrared and Raman Spectroscopy*, Academic Press, New York and London, 1964, pp. 273–274 and 189–190.
- (a) R. Mattes, H. Bierbüsse and J. Fuchs, *Z. Anorg. Allg. Chem.*, 1971, **385**, 230; (b) C. Rocchiccioli-Deltcheff, R. Thouvenot and M. Fouassier, *Inorg. Chem.*, 1982, **21**, 30.
- (a) B. Modéc, J. V. Brenčič and L. Golič, *Polyhedron*, 2000, **19**, 1219; (b) B. Modéc, J. V. Brenčič, L. Golič and L. M. Daniels, *Polyhedron*, 2000, **19**, 1407; (c) B. Modéc, J. V. Brenčič, R. C. Finn, R. S. Rarig and J. Zubieta, *Inorg. Chim. Acta*, 2001, **322**, 113; (d) B. Modéc, J. V. Brenčič, J. Zubieta and P. J. Hagrman, *Inorg. Chem. Commun.*, 2001, **4**, 537.
- C. Limberg, S. Parsons, A. J. Downs and D. J. Watkin, *J. Chem. Soc., Dalton Trans.*, 1994, 1169.
- (a) C. Limberg, S. Parsons and A. J. Downs, *J. Chem. Soc., Chem. Commun.*, 1994, 497; (b) A. J. Blake, A. J. Downs, C. Limberg and S. Parsons, *J. Chem. Soc., Dalton Trans.*, 1995, 3263.
- T. Duraisamy, A. Ramanan and J. J. Vittal, *J. Mater. Chem.*, 1999, **9**, 763; (b) P. J. Zapf, R. C. Haushalter and J. Zubieta, *Chem. Commun.*, 1997, 321.